Nonlinear Analysis: Modelling and Control, 2019, Vol. 24, No. 3, 332–352 ISSN: 1392-5113
https://doi.org/10.15388/NA.2019.3.2 eISSN: 2335-8963

Shifted Jacobi spectral collocation method with convergence analysis for solving integro-differential equations and system of integro-differential equations

Eid H. Doha[a], **Mohamed A. Abdelkawy**[b,c], **Ahmed Z.M. Amin**[d], **Dumitru Baleanu**[e,f]

[a]Department of Mathematics, Faculty of Science,
Cairo University, Giza, Egypt
eiddoha@sci.cu.edu.eg

[b]Department of Mathematics and Statistics, College of Science,
Al-Imam Mohammad Ibn Saud Islamic University (IMSIU),
Riyadh, Saudi Arabia
melkawy@yahoo.com

[c]Department of Mathematics, Faculty of Science,
Beni-Suef University, Beni-Suef, Egypt

[d]Department of Basic Science, Institute of Engineering,
Canadian International College (CIC), Giza, Egypt
azm.amin@yahoo.com

[e]Department of Mathematics, Cankaya University, Ankara, Turkey
dumitru@cankaya.edu.tr

[f]Institute of Space Sciences, Magurele-Bucharest, Romania

Received: Frbruary 26, 2018 / **Revised:** December 5, 2018 / **Published online:** April 19, 2019

Abstract. This article addresses the solution of multi-dimensional integro-differential equations (IDEs) by means of the spectral collocation method and taking the advantage of the properties of shifted Jacobi polynomials. The applicability and accuracy of the present technique have been examined by the given numerical examples in this paper. By means of these numerical examples, we ensure that the present technique is simple and very accurate. Furthermore, an error analysis is performed to verify the correctness and feasibility of the proposed method when solving IDE.

Keywords: integro-differential equation, spectral collocation method, shifted Jacobi polynomials, Jacobi–Gauss quadrature.

1 Introduction

Recently, the studies of IDEs were developed very intensively and speedily. Numerical solutions of the IDEs have received considerable attention not only in mathematics, but also in computational physics. These equations are combinations of the unknown functions that appear under the sign of integration and derivatives. In addition, IDEs are used in many problems of mechanics, engineering, chemistry, physics, biology, astronomy, potential theory, electrostatics, etc. [3, 12, 22, 25, 31–33, 37–39, 45].

In few years, many published papers (e.g., [13, 16, 31, 35]) were devoted for solving IDEs. Maleknejad et al. [30] implemented the Bernstein operational matrix to study a system of linear Volterra–Fredholm IDEs. The nonlinear IDEs were studied by means of the meshless method in [17]. Zarebnia [47] developed and proposed an efficacious numerical solution for the Volterra IDEs by using sinc method. Recently, variational iteration method were applied by Nadjafi et al. [36] to numerically solve the system of IDEs. More recently, Yüzbaşı [46] proposed the collocation approach for solving Fredholm–Volterra IDEs.

In last years, there are high level of interest of the spectral methods for solving many kinds of differential and IDEs due to their ease of application for finite and infinite domains [1, 2, 28, 34, 40, 44]. The speed of convergence is one of the great feature of the spectral method. Besides, the spectral methods have enormous rates of convergence, they also have high level of reliability. The spectral method were divided into four classifications: collocation [5, 6, 26, 27], tau [8, 20, 24, 41], Galerkin [14, 15, 23] and Petrov–Galerkin [4, 29] method. The main idea of the spectral methods is to express the solution of the problem as a finite sum of given basis of functions (orthogonal polynomials or combination of orthogonal polynomials) and then to choose the coefficients in order to minimize the difference between the exact and the numerical solutions.

Our motivation in this paper is to develop spectral approximation of IDEs. We propose the shifted Jacobi–Gauss collocation (SJGC) method to find the solution $u_N(x)$ by means of the shifted Jacobi polynomial. The IDEs is collocated at the selected points. For convenient, we use the nodes of the shifted Jacobi–Gauss (SJG) interpolation as collocation points. These equations together with the initial conditions produces a system of linear algebraic equations, which can be easily solved. This scheme is one of the most suitable methods for solving system of algebraic equations.

The outlines of the present paper are arranged as follows. We present few revelent properties of shifted Jacobi polynomials in the following section. In Section 3, we propose the SJGC scheme to solve one-dimensional IDEs. In Section 4, we solve linear two-dimensional Volterra IDEs with the initial conditions. While in Section 5, we present some useful lemmas and error analysis of the IDEs. In Section 6, several numerical examples and comparisons between our numerical results and those of other methods are discussed. Finally, Section 7 outlines the conclusions.

2 Properties of shifted Jacobi polynomials

By means of the main properties of Jacobi polynomials, we conclude the following:

$$\mathcal{P}_k^{(\alpha,\beta)}(-x) = (-1)^k \mathcal{P}_k^{(\beta,\alpha)}(x), \qquad \mathcal{P}_k^{(\alpha,\beta)}(-1) = \frac{(-1)^k \Gamma(k+\beta+1)}{k!\Gamma(\beta+1)}, \tag{1}$$

where $\alpha, \beta > -1$, $x \in [-1, 1]$.

Furthermore, the rth derivative of $\mathcal{P}_j^{(\alpha,\beta)}(x)$ is computed as

$$D^r \mathcal{P}_j^{(\alpha,\beta)}(x) = \frac{\Gamma(j+\alpha+\beta+r+1)}{2^r \Gamma(j+\alpha+\beta+1)} \mathcal{P}_{j-r}^{(\alpha+r,\beta+r)}(x),$$

where r is an integer. Let the shifted Jacobi polynomial $\mathcal{P}_{L,k}^{(\alpha,\beta)}(x)$ on the interval $[0,L]$ be denoted by $\mathcal{P}_{L,k}^{(\alpha,\beta)}(x) = \mathcal{P}_k^{(\alpha,\beta)}(2x/L-1),\ L>0$, thus

$$\begin{aligned}\mathcal{P}_{L,k}^{(\alpha,\beta)}(x) &= \sum_{j=0}^{k} (-1)^{k-j} \frac{\Gamma(k+\beta+1)\Gamma(j+k+\alpha+\beta+1)}{\Gamma(j+\beta+1)\Gamma(k+\alpha+\beta+1)(k-j)!j!L^j} x^j \\ &= \sum_{j=0}^{k} \frac{\Gamma(k+\alpha+1)\Gamma(k+j+\alpha+\beta+1)}{j!(k-j)!\Gamma(j+\alpha+1)\Gamma(k+\alpha+\beta+1)L^j} (x-L)^j.\end{aligned}$$

Thereby

$$\mathcal{P}_{L,k}^{(\alpha,\beta)}(0) = (-1)^k \frac{\Gamma(k+\beta+1)}{\Gamma(\beta+1)\,k!}, \qquad \mathcal{P}_{L,k}^{(\alpha,\beta)}(L) = \frac{\Gamma(k+\alpha+1)}{\Gamma(\alpha+1)\,k!},$$

$$\begin{aligned} D^r \mathcal{P}_{L,k}^{(\alpha,\beta)}(0) &= \frac{(-1)^{k-r}\Gamma(k+\beta+1)(k+\alpha+\beta+1)_r}{L^r \Gamma(k-r+1)\Gamma(r+\beta+1)}, \\ D^r \mathcal{P}_{L,k}^{(\alpha,\beta)}(L) &= \frac{\Gamma(k+\alpha+1)(k+\alpha+\beta+1)_r}{L^r \Gamma(k-r+1)\Gamma(r+\alpha+1)}, \\ D^r \mathcal{P}_{L,k}^{(\alpha,\beta)}(x) &= \frac{\Gamma(r+k+\alpha+\beta+1)}{L^r \Gamma(k+\alpha+\beta+1)} \mathcal{P}_{L,k-r}^{(\alpha+r,\beta+r)}(x). \end{aligned} \tag{2}$$

Taking $w_L^{(\alpha,\beta)}(x) = (L-x)^\alpha x^\beta$, we list the following inner product and norm related to the weighted space $L^2_{w_L^{(\alpha,\beta)}}[0,L]$ as

$$(u,v)_{w_L^{(\alpha,\beta)}} = \int_0^L u(x)v(x)w_L^{(\alpha,\beta)}(x)\,\mathrm{d}x, \qquad \|v\|_{w_L^{(\alpha,\beta)}} = (v,v)^{1/2}_{w_L^{(\alpha,\beta)}}.$$

A complete $L^2_{w_L^{(\alpha,\beta)}}[0,L]$-orthogonal system is consisted of a set of shifted Jacobi polynomials, where

$$\big\|\mathcal{P}_{L,k}^{(\alpha,\beta)}\big\|^2_{w_L^{(\alpha,\beta)}} = \left(\frac{L}{2}\right)^{\alpha+\beta+1} h_k^{(\alpha,\beta)} = h_{L,k}^{(\alpha,\beta)},$$

where [7, 9, 18]

$$h_k^{(\alpha,\beta)} = \frac{2^{\alpha+\beta+1}\Gamma(k+\alpha+1)\Gamma(k+\beta+1)}{(2k+\alpha+\beta+1)k!\Gamma(k+\alpha+\beta+1)}.$$

We used $x_{N,j}^{(\alpha,\beta)}$ and $\varpi_{N,j}^{(\alpha,\beta)}$, $0 \leqslant j \leqslant N$, as the nodes and Christoffel numbers of the standard Jacobi–Gauss interpolation in the interval $[-1, 1]$. For shifted Jacobi–Gauss interpolation on $[0, L]$, we find

$$x_{L,N,j}^{(\alpha,\beta)} = \frac{L}{2}\big(x_{N,j}^{(\alpha,\beta)} + 1\big),$$
$$\varpi_{L,N,j}^{(\alpha,\beta)} = \left(\frac{L}{2}\right)^{\alpha+\beta+1} \varpi_{N,j}^{(\alpha,\beta)}, \quad 0 \leqslant j \leqslant N.$$

For any positive integer N, $\phi \in S_{2N+1}[0, L]$ and by means of Jacobi–Gauss quadrature property,

$$\begin{aligned}\int_0^L (L-x)^\alpha x^\beta \phi(x)\,\mathrm{d}x &= \left(\frac{L}{2}\right)^{\alpha+\beta+1} \int_{-1}^{1} (1-x)^\alpha (1+x)^\beta \phi\left(\frac{L}{2}(x+1)\right) \mathrm{d}x \\ &= \left(\frac{L}{2}\right)^{\alpha+\beta+1} \sum_{j=0}^{N} \varpi_{N,j}^{(\alpha,\beta)} \phi\left(\frac{L}{2}\big(x_{N,j}^{(\alpha,\beta)} + 1\big)\right) \\ &= \sum_{j=0}^{N} \varpi_{L,N,j}^{(\alpha,\beta)} \phi\big(x_{L,N,j}^{(\alpha,\beta)}\big).\end{aligned}$$

3 One-dimensional IDEs

3.1 Volterra IDEs with the initial condition

In this subsection, we use the spectral collocation method to solve the following Volterra IDEs:

$$\sum_{i=0}^{m} \gamma_i u^{(i)}(x) = f(x) + \int_0^x k(x,s) u(s)\,\mathrm{d}s, \quad x \in [0, L], \tag{3}$$

subject to

$$u^{(i)}(0) = d_i, \quad i = 0, \dots, m-1, \tag{4}$$

where $k(x, s)$ and $f(x)$ are given functions and γ_i $(i = 0, \dots, m)$ are constants, while $u(x)$ is unknown function.

We using the SJGC algorithm to transform the previous IDEs into system of algebraic equations. Thus, we approximate the independent variable using the SJGC algorithm at $x_{L,N,j}^{(\theta,\vartheta)}$ nodes. The nodes are the set of points in a specified domain, where the dependent variable values are approximated. In general, the choice of the location of the nodes are optional, but taking the roots of the shifted Jacobi polynomials referred to as SJG points, gives particularly accurate solutions for the spectral methods.

Now, we outline the main step of the SJGC method for solving one-dimensional IDEs. We choose the approximate solution to be of the form

$$u_N(x) = \sum_{j=0}^{N} a_j \mathcal{P}_{L,j}^{(\theta,\vartheta)}(x). \tag{5}$$

Then

$$u_N^{(i)}(x) = \sum_{j=0}^{N} a_j \frac{\mathrm{d}^i(\mathcal{P}_{L,j}^{(\theta,\vartheta)}(x))}{\mathrm{d}x^i} = \sum_{j=0}^{N} a_j \Psi_{L,j,i}^{(\theta,\vartheta)}(x), \quad i = 1, \dots, m,$$

where

$$\Psi_{L,j,i}^{(\theta,\vartheta)}(x) = \sum_{r=0}^{j-i} C_i(j,i,\theta,\vartheta) \mathcal{P}_{L,r}^{(\theta,\vartheta)}(x).$$

Equation (3) can be written as

$$\sum_{i=0}^{m} \gamma_i \sum_{j=0}^{N} a_j \Psi_{L,j,i}^{(\theta,\vartheta)}(x) = f(x) + \int_0^x \left(k(x,s) \sum_{j=0}^{N} a_j \mathcal{P}_{L,j}^{(\theta,\vartheta)}(s)\,\mathrm{d}s \right). \tag{6}$$

In the proposed SJGC method, the residual of (6) is set to zero at $(N - m + 1)$ of SJG points. Then, adopting (5)–(6), we can be write (3) in form:

$$\begin{aligned}
&\sum_{j=0}^{N} \sum_{i=0}^{m} \gamma_i a_j \Psi_{L,j,i}^{(\theta,\vartheta)}\big(x_{L,N,n}^{(\theta,\vartheta)}\big) \\
&\quad = f\big(x_{L,N,n}^{(\theta,\vartheta)}\big) + \int_0^{x_{L,N,n}^{(\theta,\vartheta)}} \left(k\big(x_{L,N,n}^{(\theta,\vartheta)}, s\big) \sum_{j=0}^{N} a_j \mathcal{P}_{L,j}^{(\theta,\vartheta)}(s)\,\mathrm{d}s \right), \quad n = m, \dots, N.
\end{aligned}$$

Then

$$\begin{aligned}
&\sum_{j=0}^{N} a_j \left(\sum_{i=0}^{m} \gamma_i \Psi_{L,j,i}^{(\theta,\vartheta)}\big(x_{L,N,j}^{(\theta,\vartheta)}\big) - \int_0^{x_{L,N,j}^{(\theta,\vartheta)}} k\big(x_{L,N,j}^{(\theta,\vartheta)}, s\big) \mathcal{P}_{L,j}^{(\theta,\vartheta)}(s)\,\mathrm{d}s \right) \\
&\quad = f\big(x_{L,N,n}^{(\theta,\vartheta)}\big), \quad n = m, \dots, N.
\end{aligned} \tag{7}$$

Using Eqs. (5) and (4), we obtain

$$\sum_{j=0}^{N} a_j \frac{(-1)^{j-i}\Gamma(j+\vartheta+1)(j+\theta+\vartheta+1)_i}{L^i\Gamma(j-i+1)\Gamma(i+\vartheta+1)} = d_i, \quad i = 1, \dots, m. \tag{8}$$

Finally, from (7) and (8) we obtain $(N + 1)$ algebraic equations, which can be easily solved for the unknown coefficients a_j. So, $u_N(x)$ given in Eq. (5) can be estimated.

3.2 System of Volterra IDEs with the initial conditions

In the current subsection, we apply the technique discussed in Section 3.1 to solve system of Volterra IDEs in the form

$$\begin{aligned}\sum_{i=0}^{m}\gamma_i u^{(i)}(x) &= f_1(x) + \int_0^x k_1(x,s)\big(u(s)+v(s)\big)\,\mathrm{d}s,\\ \sum_{i=0}^{m}\zeta_i v^{(i)}(x) &= f_2(x) + \int_0^x k_2(x,s)\big(u(s)+v(s)\big)\,\mathrm{d}s, \quad x\in[0,L],\end{aligned}\tag{9}$$

subject to

$$u^{(i)}(0)=d_i, \quad v^{(i)}(0)=\delta_i, \quad i=0,\dots,m-1, \tag{10}$$

where $f_1(x)$, $f_2(x)$, $k_1(x,t)$ and $k_2(x,t)$ are given function, and γ_i, ζ_i ($i=0,\dots,m$) are constants, while $u(x)$, $v(x)$ are unknown functions.

In the SJGC method, the approximate solution can be introduced as a truncated shifted Jacobi series:

$$u_N(x)=\sum_{j=0}^{N}a_j\mathcal{P}_{L,j}^{(\theta,\vartheta)}(x), \qquad v_N(x)=\sum_{j=0}^{N}b_j\mathcal{P}_{L,j}^{(\theta,\vartheta)}(x), \tag{11}$$

and, in virtue of (11), we deduce that

$$u_N^{(i)}(x)=\sum_{j=0}^{N}a_j\Psi_{L,j,i}^{(\theta,\vartheta)}(x), \quad v_N^{(i)}(x)=\sum_{j=0}^{N}b_j\Psi_{L,j,i}^{(\theta,\vartheta)}(x), \quad i=1,\dots,m.$$

In the proposed SJGC method, the residual of (9) is set to be zero at $2(N-m+1)$ of SJG points, thus we find

$$\begin{aligned}&\sum_{j=0}^{N}\sum_{i=0}^{m}\gamma_i a_j\Psi_{L,j,i}^{(\theta,\vartheta)}\big(x_{L,N,n}^{(\theta,\vartheta)}\big)\\ &\quad= f\big(x_{L,N,n}^{(\theta,\vartheta)}\big)+\int_0^{x_{L,N,n}^{(\theta,\vartheta)}}\left(k_1\big(x_{L,N,n}^{(\theta,\vartheta)},s\big)\left(\sum_{j=0}^{N}a_j\mathcal{P}_{L,j}^{(\theta,\vartheta)}(s)+\sum_{j=0}^{N}b_j\mathcal{P}_{L,j}^{(\theta,\vartheta)}(s)\right)\right)\mathrm{d}s,\\ &\sum_{j=0}^{N}\sum_{i=0}^{m}\zeta_i b_j\Psi_{L,j,i}^{(\theta,\vartheta)}\big(x_{L,N,n}^{(\theta,\vartheta)}\big)\\ &\quad= f_2\big(x_{L,N,n}^{(\theta,\vartheta)}\big)+\int_0^{x_{L,N,n}^{(\theta,\vartheta)}}\left(k_2\big(x_{L,N,n}^{(\theta,\vartheta)},s\big)\left(\sum_{j=0}^{N}a_j\mathcal{P}_{L,j}^{(\theta,\vartheta)}(s)+\sum_{j=0}^{N}b_j\mathcal{P}_{L,j}^{(\theta,\vartheta)}(s)\right)\right)\mathrm{d}s,\end{aligned}\tag{12}$$

where $n = m, \dots, N$. Using (2), Eq. (10) can be reformulated as

$$\begin{aligned} &\sum_{j=0}^{N} a_j \frac{(-1)^{j-i}\Gamma(j+\vartheta+1)(j+\theta+\vartheta+1)_i}{L^i\Gamma(j-i+1)\Gamma(i+\vartheta+1)} = d_i, \quad i = 1, \dots, m, \\ &\sum_{j=0}^{N} b_j \frac{(-1)^{j-i}\Gamma(j+\vartheta+1)(j+\theta+\vartheta+1)_i}{L^i\Gamma(j-i+1)\Gamma(i+\vartheta+1)} = \delta_i, \quad i = 1, \dots, m. \end{aligned} \tag{13}$$

Equations (12) and (13) give a system of algebraic equations, which can be solved for the unknown coefficients a_j and b_j. So, $u_N(x)$ and $v_N(x)$ given in Eq. (11) can be estimated.

3.3 Mixed of Volterra–Fredholm IDEs with the initial conditions

This section present an efficient spectral algorithm by means of the SJGC method to numerically solve linear mixed Volterra–Fredholm IDEs in the form

$$\sum_{i=0}^{m} \gamma_i u^{(i)}(x) = f(x) + \int_0^x k(x,s)u(s)\,\mathrm{d}s + \int_0^L k(x,s)u(s)\,\mathrm{d}s, \quad x \in [0.L],$$

subject to

$$u^{(i)}(0) = d_i \quad i = 0, \dots, m-1.$$

Similar steps to that given in the previous subsections, enable one to write Eq. (3.3) in the form

$$\begin{aligned} \sum_{i=0}^{m} \gamma_i a_j \Psi_{L,j,i}^{(\theta,\vartheta)}(x) &= f(x) + \int_0^x k(x,s) \sum_{j=0}^{N} a_j \mathcal{P}_{L,j}^{(\theta,\vartheta)}(s)\,\mathrm{d}s \\ &\quad + \int_0^L k(x,s) \sum_{j=0}^{N} a_j \mathcal{P}_{L,j}^{(\theta,\vartheta)}(s)\,\mathrm{d}s, \quad x \in [0,L]. \end{aligned}$$

Based on the information in the previous section, we get the following system of algebraic equations:

$$\begin{aligned} \sum_{i=0}^{m} \gamma_i a_j \Psi_{L,j,i}^{(\theta,\vartheta)}\big(x_{L,N,n}^{(\theta,\vartheta)}\big) &= \int_0^{x_{L,N,n}^{(\theta,\vartheta)}} k\big(x_{L,N,n}^{(\theta,\vartheta)}, s\big) \sum_{j=0}^{N} a_j \mathcal{P}_{L,j}^{(\theta,\vartheta)}(s)\,\mathrm{d}s \\ &\quad + \int_0^L k\big(x_{L,N,n}^{(\theta,\vartheta)}, s\big) \sum_{j=0}^{N} a_j \mathcal{P}_{L,j}^{(\theta,\vartheta)}(s)\,\mathrm{d}s \\ &\quad + f\big(x_{L,N,n}^{(\theta,\vartheta)}\big), \quad n = m, \dots, N, \\ \sum_{j=0}^{N} a_j \frac{(-1)^{j-i}\Gamma(j+\vartheta+1)(j+\theta+\vartheta+1)_i}{L^i\Gamma(j-i+1)\Gamma(i+\vartheta+1)} &= d_i, \quad i = 1, \dots, m. \end{aligned}$$

The previous linear system of algebraic equations can be easily solved. After determining the coefficients a_j, it is straightforward to compute the approximate solution $u_N(x)$ at any value of $x \in [0, L]$ in the given domain from the following equation

$$u_N(x) = \sum_{j=0}^{N} a_j \mathcal{P}_{L,j}^{(\theta,\vartheta)}(x).$$

4 Two-dimensional IDEs

In this section, we extend the above analysis to solve the following two-dimensional linear Volterra IDEs:

$$\begin{aligned}&\frac{\partial^2 u(x,t)}{\partial t^2} + u(x,t)\\&\quad = f(x,t) + \int_0^t \int_0^x k(x,t,y,z) u(s,y)\,\mathrm{d}y\,\mathrm{d}z, \quad (x,t) \in [0,L] \times [0,\tau],\end{aligned} \tag{14}$$

subject to

$$u(x,0) = g_0(x), \qquad \frac{\partial u}{\partial t}(x,0) = g_1(x), \tag{15}$$

where $k(x,t,y,z)$ and $f(x,t)$ are given functions, while $u(x,t)$ is unknown function.

Therefore, the SJGC method will be applied to transform the previous two-dimensional Volterra IDEs into system of algebraic equations.

Let us expand the dependent variable in the form

$$u_{N,M}(x,t) = \sum_{i=0}^{M} \sum_{j=0}^{N} a_{ij} \mathcal{P}_{\tau,i}^{(\theta_2,\vartheta_2)}(t) \mathcal{P}_{L,j}^{(\theta_1,\vartheta_1)}(x). \tag{16}$$

The partial derivatives of the approximate solution $u_{N,M}(x,t)$ is then estimated as

$$\begin{aligned}\frac{\partial u_{N,M}(x,t)}{\partial t} &= \sum_{i=0}^{N} \sum_{j=0}^{M} a_{i,j} \phi_{i,j}(x,t),\\ \frac{\partial^2 u_{N,M}(x,t)}{\partial t^2} &= \sum_{i=0}^{N} \sum_{j=0}^{M} a_{i,j} \varphi_{i,j}(x,t),\end{aligned} \tag{17}$$

where

$$\begin{aligned}\phi_{i,j}(x,t) &= \frac{\mathrm{d}\mathcal{P}_{\tau,i}^{(\theta_2,\vartheta_2)}(t)}{\mathrm{d}t} \mathcal{P}_{L,j}^{(\theta_1,\vartheta_1)}(x),\\ \varphi_{i,j}(x,t) &= \frac{\mathrm{d}^2\mathcal{P}_{\tau,i}^{(\theta_2,\vartheta_2)}(t)}{\mathrm{d}t^2} \mathcal{P}_{L,j}^{(\theta_1,\vartheta_1)}(x).\end{aligned}$$

From (14), (16) and (17) we can write Eq. (14) as

$$\sum_{i=0}^{N}\sum_{j=0}^{M} a_{i,j}\varphi_{i,j}(x,t) = \int_0^t\int_0^x k(x,t,y,z)\sum_{i=0}^{M}\sum_{j=0}^{N} a_{ij}\mathcal{P}_{\tau,i}^{(\theta_2,\vartheta_2)}(z)\mathcal{P}_{L,j}^{(\theta_1,\vartheta_1)}(y)\,\mathrm{d}y\,\mathrm{d}z + f(x,t) - \sum_{i=0}^{M}\sum_{j=0}^{N} a_{ij}\mathcal{P}_{\tau,i}^{(\theta_2,\vartheta_2)}(t)\mathcal{P}_{L,j}^{(\theta_1,\vartheta_1)}(x), \quad (x,t)\in[0,L]\times[0,\tau]. \tag{18}$$

In the proposed SJGC algorithm, the residual of (18) is set to zero at $(N+1)(M-1)$ of SJC point. Furthermore, the initial conditions in (15) will be collocated at SJG points. Firstly, we have $(N+1)(M-1)$ algebraic equations for $(M+1)(N+1)$ unknown of $a_{i,j}$

$$\sum_{i=0}^{N}\sum_{j=0}^{M} a_{i,j}\varphi_{i,j}\big(x_{L,N,l}^{(\theta_1,\vartheta_1)},t_{L,N,m}^{(\theta_2,\vartheta_2)}\big) = \int_0^{t_{L,N,m}^{(\theta_2,\vartheta_2)}}\int_0^{x_{L,N,l}^{(\theta_1,\vartheta_1)}} k\big(x_{L,N,l}^{(\theta_1,\vartheta_1)},t_{L,N,m}^{(\theta_2,\vartheta_2)},y,z\big)\sum_{i=0}^{M}\sum_{j=0}^{N} a_{ij}\mathcal{P}_{\tau,i}^{(\theta_2,\vartheta_2)}(z)\mathcal{P}_{L,j}^{(\theta_1,\vartheta_1)}(y)\,\mathrm{d}y\,\mathrm{d}z + f\big(x_{L,N,l}^{(\theta_1,\vartheta_1)},t_{L,N,m}^{(\theta_2,\vartheta_2)}\big) - \sum_{i=0}^{M}\sum_{j=0}^{N} a_{ij}\mathcal{P}_{\tau,i}^{(\theta_2,\vartheta_2)}\big(t_{L,N,m}^{(\theta_2,\vartheta_2)}\big)\mathcal{P}_{L,j}^{(\theta_1,\vartheta_1)}\big(x_{L,N,l}^{(\theta_1,\vartheta_1)}\big),$$

$l=0,\dots,N$, $m=1,\dots,M-1$. The previous equations can be rearranging as

$$\sum_{i=0}^{M}\sum_{j=0}^{N} a_{ij}\eta_{i,j}^{l,m} = f\big(x_{L,N,l}^{(\theta_1,\vartheta_1)},t_{L,N,m}^{(\theta_2,\vartheta_2)}\big), \quad l=0,\dots,N,\ m=0,\dots,M,$$

where

$$\eta_{i,j}^{l,m} = \varphi_{i,j}\big(x_{L,N,l}^{(\theta_1,\vartheta_1)},t_{L,N,m}^{(\theta_2,\vartheta_2)}\big) - \int_0^{t_{L,N,m}^{(\theta_2,\vartheta_2)}}\int_0^{x_{L,N,l}^{(\theta_1,\vartheta_1)}} k\big(x_{L,N,l}^{(\theta_1,\vartheta_1)},t_{L,N,m}^{(\theta_2,\vartheta_2)},y,z\big)\mathcal{P}_{\tau,i}^{(\theta_2,\vartheta_2)}(z)\mathcal{P}_{L,j}^{(\theta_1,\vartheta_1)}(y)\,\mathrm{d}y\,\mathrm{d}z + \mathcal{P}_{\tau,i}^{(\theta_2,\vartheta_2)}\big(t_{L,N,m}^{(\theta_2,\vartheta_2)}\big)\mathcal{P}_{L,j}^{(\theta_1,\vartheta_1)}\big(x_{L,N,l}^{(\theta_1,\vartheta_1)}\big).$$

Combining Eqs. (16) and (17), we obtain

$$\sum_{i=0}^{N}\sum_{j=0}^{M} a_{i,j}\mathcal{P}_{\tau,i}^{(\theta_2,\vartheta_2)}(0)\mathcal{P}_{L,j}^{(\theta_1,\vartheta_1)}\big(x_{L,N,l}^{(\theta_1,\vartheta_1)}\big) = g_0\big(x_{L,N,l}^{(\theta_1,\vartheta_1)}\big), \quad l=0,\dots,N,$$
$$\sum_{i=0}^{N}\sum_{j=0}^{M} a_{i,j}D_t\mathcal{P}_{\tau,i}^{(\theta_2,\vartheta_2)}(0)\mathcal{P}_{L,j}^{(\theta_1,\vartheta_1)}\big(x_{L,N,l}^{(\theta_1,\vartheta_1)}\big) = g_1\big(x_{L,N,l}^{(\theta_1,\vartheta_1)}\big), \quad l=0,\dots,N,$$

finally, the linear system of $(N+1)(M+1)$ algebraic equations produced automatically and can be easily solved. Therefore, $u_{N,M}(x,t)$ can be determined in closed form.

5 Lemmas and error analysis

Some useful lemmas and a discussion about the error analysis of the algorithm presented in Section 3.1.

5.1 Lemmas

Definition 1. Let $P_N : L^2(I) \to X_N$ be the L^2 orthogonal projection, defined by

$$(P_N u - u,\, v) = 0 \quad \forall v \in X_N.$$

Definition 2. Some weighted Hilbert spaces will be presented here.

For a nonnegative integer m, define [10, 11, 42]

$$H^m_{w^{\alpha,\beta}}(-1,1) = \big\{v\colon\, \partial_x^i v \in L^2_{w^{\alpha,\beta}}(-1,1),\ 0 \leqslant i \leqslant m\big\},$$

where $\partial_x^i v(x) = \partial^i v(x)/\partial x^i$ related to the following seminorm and the norm:

$$|v|_{m,w^{\alpha,\beta}} = \big\|\partial_x^m v\big\|_{w^{\alpha,\beta}},$$
$$\|v\|_{m,w^{\alpha,\beta}} = \left(\sum_{i=0}^{m}\big\|\partial_x^i v\big\|^2_{w^{\alpha,\beta}}\right)^{1/2}.$$

Lemma 1. *Assume that* $u \in H^m(I)$, $I \equiv (-1,1)$. *The interpolation of* u ($I_N^{\alpha,\beta}u$) *computed at any points of Jacobi–Gauss points* (*Gauss or Gauss–Radau or Gauss–Lobatto points*) *stasifies the following estimates* [11]:

$$\big\|u - I_N^{\alpha,\beta}u\big\|_{L^2_{w^{\alpha,\beta}}(I)} \leqslant CN^{-m}|u|_{H^{m,N}_{w^{\alpha,\beta}}(I)},$$
$$\big\|u - I_N^{\alpha,\beta}u\big\|_{L_\infty(I)} \leqslant CN^{1/2-m}|u|_{H^{m,N}_{w^{\alpha,\beta}}(I)},$$
$$\big\|u'(x) - \big(I_N^{\alpha,\beta}u(x)\big)'\big\|_{L^2_{w^{\alpha,\beta}}(I)} \leqslant CN^{1-m}|u|_{H^{m,N}_{w^{\alpha,\beta}}(I)}.$$

5.2 Error analysis

The main goal is to estimate the accuracy of the solutions we obtained. In this section, error analysis for the introduced technique (3) will be discussed. We provided error analysis for the proposed method to indicate its exponential rate of convergence, provided that the source and kernel functions are sufficiently smooth. In order to do that, some properties of Banach algebras and Sobolev inequality are taken into account.

Theorem 1. *Let* $u(x)$ *the exact solution of the Volterra IDEs* (3) *and assume that* $I_N^{\alpha,\beta}(u(x)) = u_N(x)$ *be the spectral collection approximation defined by Eq.* (7)*, therefore, we have*

$$\begin{aligned}\big\|u(x) - u_N(x)\big\|_{L^2_{w^{\alpha,\beta}}(I)} \leqslant CN^{-m}\big(&N|u|_{H^{m,N}_{w^{\alpha,\beta}}(I)} + \gamma N^{1/2}|u|_{H^{m,N}_{w^{\alpha,\beta}}(I)} \\ &+ |f|_{H^{m,N}_{w^{\alpha,\beta}}(I)} + \big|k(x,s)\big|_{H^{m,N}_{w^{\alpha,\beta}}(I)}\|u\|_{L^2_{w^{\alpha,\beta}}(I)}\big).\end{aligned}$$

Proof. Let the equation of linear Volterra IDEs in (3), where $m = 1$,

$$\begin{aligned} u'(x) + u(x) &= f(x) + \int_0^x k(x,s)u(s)\,\mathrm{d}s, \\ u(x) &= -u'(x) + f(x) + \int_0^x k(x,s)u(s)\,\mathrm{d}s, \end{aligned} \tag{19}$$

while using the approximate solution, we have

$$\begin{aligned} \big(I_N^{\alpha,\beta}u(x)\big)' + u_N(x) &= I_N^{\alpha,\beta}f(x) + \int_0^{x^{(\theta,\vartheta)}_{L,N,n}} I^{\alpha,\beta}_{N,N}k\big(x^{(\theta,\vartheta)}_{L,N,n},s\big)I_N^{\alpha,\beta}u(s)\,\mathrm{d}s, \\ u_N(x) &= -\big(I_N^{\alpha,\beta}u(x)\big)' + I_N^{\alpha,\beta}f(x) + \int_0^{x^{(\theta,\vartheta)}_{L,N,n}} I^{\alpha,\beta}_{N,N}k\big(x^{(\theta,\vartheta)}_{L,N,n},s\big)I_N^{\alpha,\beta}u(s)\,\mathrm{d}s. \end{aligned} \tag{20}$$

Subtracting (20) from (19), we get

$$\begin{aligned} u(x) - u_N(x) = {} & \big(\big(I_N^{\alpha,\beta}u(x)\big)' - u'(x)\big) + \big(f(x) - I_N^{\alpha,\beta}f(x)\big) \\ & + \int_0^{x^{(\theta,\vartheta)}_{L,N,n}} k\big(x^{(\theta,\vartheta)}_{L,N,n},s\big)u(s)\,\mathrm{d}s \\ & - \int_0^{x^{(\theta,\vartheta)}_{L,N,n}} I^{\alpha,\beta}_{N,N}\big(k\big(x^{(\theta,\vartheta)}_{L,N,n},s\big)\big)I_N^{\alpha,\beta}u(s)\,\mathrm{d}s, \end{aligned}$$

then

$$
\begin{aligned}
e_N(x) = {} & \big(\big(I_N^{\alpha,\beta} u(x)\big)' - u'(x)\big) + \big(f(x) - I_N^{\alpha,\beta} f(x)\big) \\
& + \int_0^{x_{L,N,n}^{(\theta,\vartheta)}} e_{N,N} k\big(x_{L,N,n}^{(\theta,\vartheta)}, s\big) I_N^{\alpha,\beta} u(s)\,\mathrm{d}s \\
& + \int_0^{x_{L,N,n}^{(\theta,\vartheta)}} \big(k\big(x_{L,N,n}^{(\theta,\vartheta)}, s\big)\big) u(s)\,\mathrm{d}s \\
& - \int_0^{x_{L,N,n}^{(\theta,\vartheta)}} k\big(x_{L,N,n}^{(\theta,\vartheta)}, s\big) I_N^{\alpha,\beta} u(s)\,\mathrm{d}s, \\
e_N(x) = {} & \big(\big(I_N^{\alpha,\beta} u(x)\big)' - u'(x)\big) + \big(f(x) - I_N^{\alpha,\beta} f(x)\big) \\
& + \int_0^{x_{L,N,n}^{(\theta,\vartheta)}} e_{N,N} k\big(x_{L,N,n}^{(\theta,\vartheta)}, s\big) I_N^{\alpha,\beta} u(s)\,\mathrm{d}s \\
& + \int_0^{x_{L,N,n}^{(\theta,\vartheta)}} k\big(x_{L,N,n}^{(\theta,\vartheta)}, s\big)\big(u(s) - I_N^{\alpha,\beta} u(s)\big)\,\mathrm{d}s,
\end{aligned}
$$

where $e_{N,N} = k(x_{L,N,n}^{(\theta,\vartheta)}, s) - I_{N,N}^{\alpha,\beta}(k(x_{L,N,n}^{(\theta,\vartheta)}, s))$. Then

$$e_N(x) = J_1 + J_2 + J_3 + J_4$$

$$
\begin{aligned}
J_1 &= \big(I_N^{\alpha,\beta} u(x)\big)' - u'(x), & J_2 &= \int_0^{x_{L,N,n}^{(\theta,\vartheta)}} k\big(x_{L,N,n}^{(\theta,\vartheta)}, s\big)\big(u(s) - I_N^{\alpha,\beta} u(s)\big)\,\mathrm{d}s, \\
J_3 &= f(x) - I_N^{\alpha,\beta} f(x), & J_4 &= \int_0^{x_{L,N,n}^{(\theta,\vartheta)}} e_{N,N} k\big(x_{L,N,n}^{(\theta,\vartheta)}, s\big) I_N^{\alpha,\beta} u(s)\,\mathrm{d}s.
\end{aligned}
$$

From Gronwall inequality [43] we can write

$$\big\|e_N(x)\big\|_{L^2_{w^{\alpha,\beta}}} \leqslant \|J_1\|_{L^2_{w^{\alpha,\beta}}} + \|J_2\|_{L^2_{w^{\alpha,\beta}}} + \|J_3\|_{L^2_{w^{\alpha,\beta}}} + \|J_4\|_{L^2_{w^{\alpha,\beta}}}. \tag{21}$$

From Lemma 1 [11] we can write

$$\|J_1\|_{L^2_{w^{\alpha,\beta}}(I)} = \big\|\big(I_N^{\alpha,\beta} u(x)\big)'(x) - u'(x)\big\| \leqslant C_1 N^{1-m} |u|_{H^{m,N}_{w^{\alpha,\beta}}(I)}. \tag{22}$$

$$
\begin{aligned}
\|J_2\|_{L^2_{w^{\alpha,\beta}}(I)} &= \left\| \int\limits_0^{x^{(\theta,\vartheta)}_{L,N,n}} k\big(x^{(\theta,\vartheta)}_{L,N,n}, s\big)\big(u(s) - I^{\alpha,\beta}_N u(s)\big)\,\mathrm{d}s \right\|_{L^2_{w^{\alpha,\beta}}(I)} \\
&\leqslant \left\| \int\limits_0^{x^{(\theta,\vartheta)}_{L,N,n}} k\big(x^{(\theta,\vartheta)}_{L,N,n}, s\big)\big(u(s) - I^{\alpha,\beta}_N u(s)\big)\,\mathrm{d}s \right\|_{\infty} \\
&\leqslant \gamma \big\|\big(u(s) - I^{\alpha,\beta}_N u(s)\big)\big\|_{\infty},
\end{aligned}
$$

where the value of γ is given as [19]

$$
\gamma = \max_{a \leqslant x^{(\theta,\vartheta)}_{L,N,n} \leqslant b} \big|k(x,s)\big|.
$$

Therefore from Lemma 1 [11]

$$
\|J_2\|_{L^2_{w^{\alpha,\beta}}(I)} \leqslant \gamma C_2 N^{1/2-m} |u|_{H^{m,N}_{w^{\alpha,\beta}}(I)}. \tag{23}
$$

From Lemma 1 [11] and [21] we can write

$$
\|J_3\|_{L^2_{w^{\alpha,\beta}}(I)} = \big\|f - I^{\alpha,\beta}_N f\big\| \leqslant C_3 N^{-m} |f|_{H^{m,N}_{w^{\alpha,\beta}}(I)}. \tag{24}
$$

Finally, by using Cauchy–Schwartz inequality we write

$$
\|J_4\|_{L^2_{w^{\alpha,\beta}}} \leqslant \big\|e_{N,N} k\big(x^{(\theta,\vartheta)}_{L,N,n}, s\big)\big\|_{L^2_{w^{\alpha,\beta}}} \big\|I^{\alpha,\beta}_N u(s)\big\|_{L^2_{w^{\alpha,\beta}}}. \tag{25}
$$

Now from [11, 19] we have

$$
\begin{aligned}
\big\|e_{N,N} k\big(x^{(\theta,\vartheta)}_{L,N,n}, s\big)\big\|_{L^2_{w^{\alpha,\beta}}(I)} &\leqslant \big\|k\big(x^{(\theta,\vartheta)}_{L,N,n}, s\big) - I^{\alpha,\beta}_{N,N} k\big(x^{(\theta,\vartheta)}_{L,N,n}, t\big)\big\|_{L^2_{w^{\alpha,\beta}}(I)} \\
&\leqslant C_4 N^{-m} \big|k(x,s)\big|_{H^{m,N}_{w^{\alpha,\beta}}(I)}.
\end{aligned} \tag{26}
$$

Now an upper bound for (25) follows from (26) and using equation (5.5.3) in [11]:

$$
\|J_4\|_{L^2_{w^{\alpha,\beta}}(I)} \leqslant \big(C_4 N^{-m} |k(x,s)|_{H^{m,N}_{w^{\alpha,\beta}}(I)}\big)\big(C_5 \|u\|_{L^2_{w^{\alpha,\beta}}(I)}\big).
$$

Then

$$
\|J_4\|_{L^2_{w^{\alpha,\beta}}(I)} \leqslant C_6 N^{-m} \big|k(x,s)\big|_{H^{m,N}_{w^{\alpha,\beta}}(I)} \|u\|_{L^2_{w^{\alpha,\beta}}(I)}. \tag{27}
$$

From Eqs. (21)–(24), (27),

$$
\begin{aligned}
&\big\|u(x) - u_N(x)\big\|_{L^2_{w^{\alpha,\beta}}(I)} \\
&\quad \leqslant C_1 N^{1-m} |u|_{H^{m,N}_{w^{\alpha,\beta}}(I)} + \gamma C_2 N^{1/2-m} |u|_{H^{m,N}_{w^{\alpha,\beta}}(I)} + C_3 N^{-m} |f|_{H^{m,N}_{w^{\alpha,\beta}}(I)} \\
&\qquad + C_6 N^{-m} \big|k(x,s)\big|_{H^{m,N}_{w^{\alpha,\beta}}(I)} \|u\|_{L^2_{w^{\alpha,\beta}}(I)}.
\end{aligned}
$$

Then

$$\begin{aligned}
&\|u(x)-u_N(x)\|_{L^2_{w^{\alpha,\beta}}(I)} \\
&\quad\leqslant N^{-m}\bigl(C_1N|u|_{H^{m,N}_{w^{\alpha,\beta}}(I)} +_2 \gamma N^{1/2}|u|_{H^{m,N}_{w^{\alpha,\beta}}(I)} + C_3|f|_{H^{m,N}_{w^{\alpha,\beta}}(I)} \\
&\qquad + C_6\bigl|k(x,s)\bigr|_{H^{m,N}_{w^{\alpha,\beta}}(I)}\|u\|_{L^2_{w^{\alpha,\beta}}(I)}\bigr),
\end{aligned}$$

the proof is complete. □

6 Numerical results

We listed several examples to illustrate the powerful and effectiveness of the proposed method. The mentioned comparisons of the numerical results detect that the previous algorithms are very appropriate and effective.

The difference between the exact solution and the value of the approximate solution is define as the absolute error (AE) given by

$$E(x) = \bigl|u(x) - u_N(x)\bigr|,$$

where $u(x)$ and $u_N(x)$ are the exact solution and the approximate solutions at the point x, respectively. Moreover, the maximum absolute errors (MAE) is given by

$$\mathrm{MAE} = \max\bigl\{E(x)\colon\ x \in [0, L]\bigr\}.$$

Example 1. Firstly, we introduce the linear Volterra IDEs in the form [47]

$$\begin{aligned}
u'(x) - u(x) = \int_0^x \frac{x}{1+s}u(s)\,\mathrm{d}s - \ln(1+x)\left(\frac{x}{2}\ln(1+x)+1\right) \\
+ \frac{1}{1+x}, \quad x \in [0,1],
\end{aligned}$$

with the initial condition

$$u(0) = 0,$$

knowing that the exact solution given by $u(x) = \ln(x+1)$.

A comparison between the MAE using the proposed method and the sinc method [47] is summarized in Table 1 with several choices of θ and ϑ. The numerical results presented in the Table 1 show that results are vary accurate for small value of N.

Figure 1 compares graphically the curves of numerical and exact solutions of problem (1). Moreover, we represent the logarithmic graphs of M_E (i.e., $\log_{10} M_E$) obtained by the novel algorithm with different values of N in Fig. 2.

Table 1. The MAE for Example 1.

N	Method [47]	Our method			
		N	$\theta=\vartheta=-1/2$	$\theta=\vartheta=0$	$\theta=0,\ \vartheta=1/2$
5	$1.75\cdot10^{-3}$	2	$7.02\cdot10^{-2}$	$6.93\cdot10^{-2}$	$7.59\cdot10^{-2}$
10	$1.06\cdot10^{-4}$	4	$2.72\cdot10^{-3}$	$3.20\cdot10^{-3}$	$4.32\cdot10^{-3}$
20	$1.85\cdot10^{-6}$	6	$8.00\cdot10^{-5}$	$1.10\cdot10^{-4}$	$1.70\cdot10^{-4}$
30	$8.03\cdot10^{-8}$	8	$2.34\cdot10^{-6}$	$3.63\cdot10^{-6}$	$6.23\cdot10^{-6}$
40	$5.87\cdot10^{-9}$	10	$6.86\cdot10^{-8}$	$1.17\cdot10^{-7}$	$2.20\cdot10^{-7}$
50	$5.80\cdot10^{-10}$	12	$2.01\cdot10^{-9}$	$3.73\cdot10^{-9}$	$7.54\cdot10^{-9}$
60	$7.09\cdot10^{-11}$	14	$5.90\cdot10^{-11}$	$1.18\cdot10^{-10}$	$2.53\cdot10^{-10}$
70	$1.02\cdot10^{-11}$	15	$1.01\cdot10^{-11}$	$2.08\cdot10^{-11}$	$4.62\cdot10^{-11}$
80	$1.67\cdot10^{-12}$	16	$1.73\cdot10^{-12}$	$3.67\cdot10^{-12}$	$8.38\cdot10^{-12}$
90	$3.09\cdot10^{-13}$	18	$5.10\cdot10^{-14}$	$1.14\cdot10^{-13}$	$2.74\cdot10^{-13}$
100	$6.26\cdot10^{-14}$	20	$1.66\cdot10^{-15}$	$3.78\cdot10^{-15}$	$9.10\cdot10^{-15}$

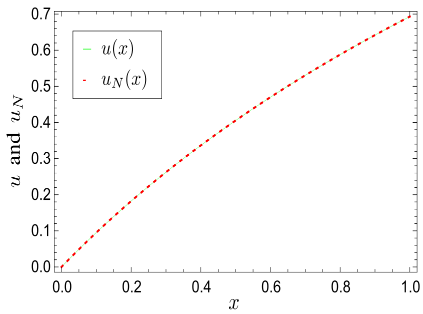

Figure 1. Comparison between the approximate $u_N(x)$ and the exact $u(x)$ solutions of Example 1 for $N=20$, $\theta=\vartheta=-1/2$.

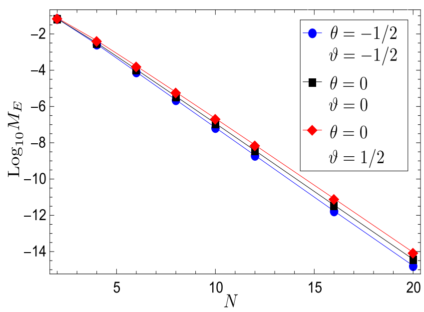

Figure 2. M_E convergence for Example 1.

Example 2. Let us, consider the system Volterra IDEs in the form [30]

$$\begin{aligned} &u_1''(x)+2xu_1'(x)-u_1(x)-\int_0^x \big(u_1(s)-u_2(s)\big)\,\mathrm{d}s \\ &\quad= 2+x-\mathrm{e}^x+2x\mathrm{e}^x-\cos(x), \\ &u_2''(x)+u_2'(x)-2xu_2(x)-\int_0^x \big(u_1(s)+u_2(s)\big)\,\mathrm{d}s \\ &\quad= 2\cos(x)-3x-(1+2x)\sin(x)-\mathrm{e}^x, \quad x\in[0,1], \end{aligned}$$

with the condition

$$u_1(0)=1,\quad u_1'(0)=1,\qquad u_2(0)=1,\quad u_2'(0)=1,$$

knowing that the exact solution given by $u_1(x)=\mathrm{e}^x$ and $u_2(x)=1+\sin(x)$.

Table 2. The AE for Example 2.

x	$u_1(x)$			$u_2(x)$		
Bernstein operational matrix [30]						
	$N=5$	$N=10$	–	$N=5$	$N=10$	–
0	$8.88\cdot10^{-16}$	$8.88\cdot10^{-16}$	–	$7.77\cdot10^{-16}$	$8.88\cdot10^{-16}$	–
0.1	$6.75\cdot10^{-7}$	$1.49\cdot10^{-13}$	–	$1.45\cdot10^{-7}$	$9.03\cdot10^{-14}$	–
0.2	$1.36\cdot10^{-6}$	$2.88\cdot10^{-13}$	–	$2.87\cdot10^{-7}$	$1.66\cdot10^{-13}$	–
0.3	$1.82\cdot10^{-6}$	$4.28\cdot10^{-13}$	–	$3.61\cdot10^{-7}$	$2.37\cdot10^{-13}$	–
0.4	$2.42\cdot10^{-6}$	$5.64\cdot10^{-13}$	–	$4.55\cdot10^{-7}$	$3.02\cdot10^{-13}$	–
0.5	$3.04\cdot10^{-6}$	$6.97\cdot10^{-13}$	–	$5.50\cdot10^{-7}$	$3.63\cdot10^{-13}$	–
0.6	$3.32\cdot10^{-6}$	$8.28\cdot10^{-13}$	–	$5.64\cdot10^{-7}$	$4.22\cdot10^{-13}$	–
0.7	$4.35\cdot10^{-6}$	$9.52\cdot10^{-13}$	–	$7.67\cdot10^{-7}$	$4.76\cdot10^{-13}$	–
0.8	$1.21\cdot10^{-5}$	$1.10\cdot10^{-12}$	–	$2.69\cdot10^{-6}$	$5.43\cdot10^{-13}$	–
0.9	$4.27\cdot10^{-5}$	$4.45\cdot10^{-13}$	–	$1.06\cdot10^{-5}$	$3.43\cdot10^{-13}$	–
1.0	$1.30\cdot10^{-4}$	$3.09\cdot10^{-11}$	–	$3.36\cdot10^{-5}$	$1.74\cdot10^{-11}$	–
Our method for $\theta=\vartheta=-1/2$						
x	$u_1(x)$			$u_2(x)$		
	$N=5$	$N=10$	$N=12$	$N=5$	$N=10$	$N=12$
0	0	0	0	0	0	0
0.1	$5.60\cdot10^{-8}$	$1.28\cdot10^{-15}$	$1.07\cdot10^{-16}$	$1.03\cdot10^{-8}$	$8.74\cdot10^{-16}$	$6.94\cdot10^{-17}$
0.2	$2.97\cdot10^{-7}$	$2.60\cdot10^{-16}$	$3.45\cdot10^{-17}$	$5.28\cdot10^{-8}$	$1.11\cdot10^{-16}$	$2.22\cdot10^{-16}$
0.3	$2.00\cdot10^{-7}$	$8.12\cdot10^{-15}$	$9.97\cdot10^{-18}$	$2.32\cdot10^{-8}$	$5.16\cdot10^{-15}$	$1.67\cdot10^{-16}$
0.4	$3.29\cdot10^{-7}$	$7.17\cdot10^{-15}$	$1.71\cdot10^{-16}$	$9.79\cdot10^{-8}$	$5.16\cdot10^{-15}$	$1.67\cdot10^{-16}$
0.5	$4.16\cdot10^{-7}$	$1.09\cdot10^{-14}$	$9.15\cdot10^{-17}$	$1.14\cdot10^{-7}$	$6.27\cdot10^{-15}$	$5.55\cdot10^{-17}$
0.6	$9.78\cdot10^{-7}$	$1.60\cdot10^{-14}$	$1.24\cdot10^{-16}$	$2.23\cdot10^{-7}$	$9.88\cdot10^{-15}$	$1.11\cdot10^{-16}$
0.7	$2.76\cdot10^{-6}$	$3.43\cdot10^{-14}$	$2.56\cdot10^{-16}$	$6.60\cdot10^{-7}$	$2.16\cdot10^{-15}$	$1.11\cdot10^{-16}$
0.8	$2.27\cdot10^{-6}$	$8.32\cdot10^{-14}$	$3.57\cdot10^{-16}$	$5.85\cdot10^{-7}$	$4.82\cdot10^{-14}$	0
0.9	$3.32\cdot10^{-5}$	$2.01\cdot10^{-13}$	$4.55\cdot10^{-16}$	$8.42\cdot10^{-6}$	$1.15\cdot10^{-13}$	$1.11\cdot10^{-16}$
1.0	$1.29\cdot10^{-4}$	$8.63\cdot10^{-12}$	$5.10\cdot10^{-15}$	$3.31\cdot10^{-5}$	$4.85\cdot10^{-12}$	$3.00\cdot10^{-15}$

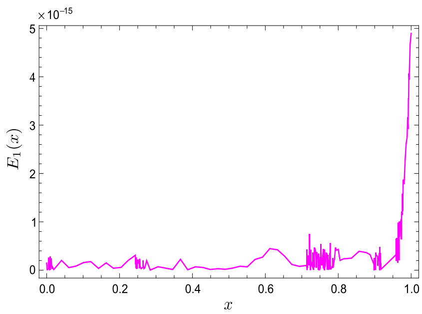

Figure 3. AE curve of $u_1(x)$ versus x in Example 2 for $N=12$ and $\theta=\vartheta=-1/2$.

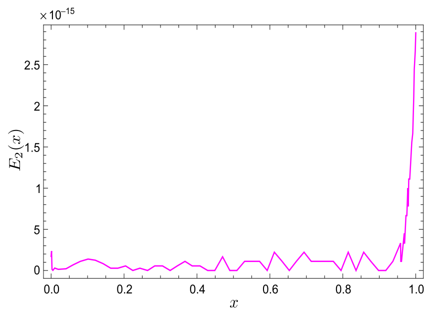

Figure 4. AE curve of $u_2(x)$ versus x in Example 2 for $N=12$ and $\theta=\vartheta=-1/2$.

Applying the technique described in Section 3.2 with different choice of N, the present method is more accurate than Bernstein operational matrix [30], see Table 2. The curves of the AE E_1 (AE of u_1) and $E_2(x)$ (AE of u_2) of Example 2 for $N=12$, are displayed in Figs. 3 and 4, respectively. In Fig. 5, we depict the logarithmic graphs of the MAE (i.e., $\log_{10} M_1$, $\log_{10} M_2$) for various values of N. This demonstrates that the new algorithm provides accuracy approximation and product exponential convergence rates.

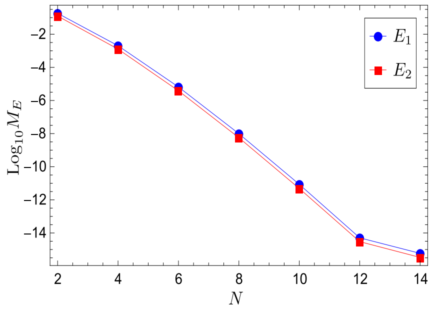

Figure 5. M_E convergence for Example 2.

Example 3. Consider the following mixed Volterra–Fredholm IDEs in the form [46]

$$u''(x) + xu'(x) - xu(x) = \mathrm{e}^x - \sin x + \frac{1}{2} x \cos x + \int_0^1 \sin x\, \mathrm{e}^{-s} u(s)\, \mathrm{d}s - \frac{1}{2} \int_0^x \cos x\, \mathrm{e}^{-s} u(s)\, \mathrm{d}s,$$

where $x \in [0, L]$, with the initial condition

$$u(0) = 1, \qquad u'(0) = 1,$$

knowing that the exact solution is given by $u(x) = \mathrm{e}^x$.

In order to confirm the high accuracy of the novel algorithm for mixed Volterra–Fredholm IDEs problem, Table 3 introduce a comparison between the maximum absolute errors obtained in [46] and the results obtained in this paper with various choices of N. We observed that a good approximation of the mixed Volterra–Fredholm IDEs is achieved for small of N.

In Fig. 6, we see the matching of the value of the AE in these figures and find in Table 3. Moreover, we represent the logarithmic graphs of M_E (i.e., $\log_{10} M_E$) obtained by the proposed method with several values of N in Fig. 7.

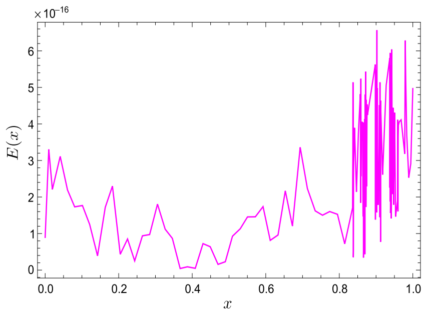

Figure 6. AE curve versus x in Example 3 for $N = 14$ and $\theta = 0$, $\vartheta = -1/2$.

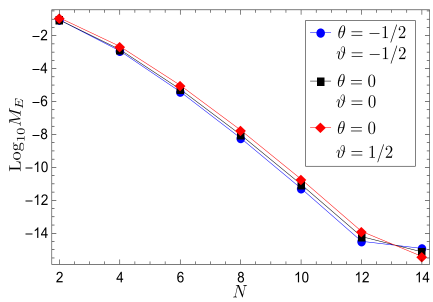

Figure 7. M_E convergence for Example 3.

Table 3. MAE for Example 3.

N	Our method	Method [47] $\theta=-1/2, \vartheta=1/2$	$\theta=\vartheta=0$	$\theta=0, \vartheta=1/2$
3	$2.37\cdot10^{-2}$	$1.54\cdot10^{-2}$	$1.80\cdot10^{-2}$	$2.35\cdot10^{-2}$
7	$1.21\cdot10^{-6}$	$1.72\cdot10^{-7}$	$2.63\cdot10^{-7}$	$4.70\cdot10^{-7}$
10	$8.23\cdot10^{-10}$	$5.32\cdot10^{-12}$	$9.28\cdot10^{-12}$	$1.94\cdot10^{-11}$
14	–	$1.21\cdot10^{-15}$	$7.43\cdot10^{-16}$	$3.93\cdot10^{-16}$

Example 4. Finally, we consider the two-dimensional Volterra IDEs

$$\frac{\partial^2 u(x,t)}{\partial t^2} + u(x,t) = f(x,t) + \int_0^t \int_0^x (\sin x + \cos t + 2y\cos z)^2 u(y,z)\,\mathrm{d}y\,\mathrm{d}z,$$

where $(x,t)\in[0,1]\times[0,1]$, subject to

$$u(x,0)=0, \qquad \frac{\partial u}{\partial t}(x,0)=x,$$

the $f(x,t)$ is given such that the exact solution is $u(x)=x\sin(t)$.

Table 4 lists the AE for several choices of N and M of Example 4. We observed a good approximation of linear two-dimensional space Volterra IDEs. The AE for Example 4 was displayed in Fig. 8 for $N=M=8$.

Table 4. AE for Example 4.

(x,t)	$N=M=2$	$N=M=4$	$N=M=6$	$N=M=8$
$(0,0)$	0	0	0	0
$(0.1,0.1)$	$1.49\cdot10^{-4}$	$2.45\cdot10^{-6}$	$7.33\cdot10^{-9}$	$9.35\cdot10^{-12}$
$(0.2,0.2)$	$1.07\cdot10^{-3}$	$1.19\cdot10^{-5}$	$2.74\cdot10^{-8}$	$3.11\cdot10^{-11}$
$(0.3,0.3)$	$3.17\cdot10^{-3}$	$2.62\cdot10^{-5}$	$5.42\cdot10^{-8}$	$7.61\cdot10^{-11}$
$(0.4,0.4)$	$6.50\cdot10^{-3}$	$4.13\cdot10^{-5}$	$9.98\cdot10^{-8}$	$1.36\cdot10^{-10}$
$(0.5,0.5)$	$1.07\cdot10^{-2}$	$5.83\cdot10^{-5}$	$1.67\cdot10^{-7}$	$1.96\cdot10^{-10}$
$(0.6,0.6)$	$1.53\cdot10^{-2}$	$8.34\cdot10^{-5}$	$2.35\cdot10^{-7}$	$2.85\cdot10^{-10}$
$(0.7,0.7)$	$1.81\cdot10^{-2}$	$1.50\cdot10^{-4}$	$3.35\cdot10^{-7}$	$4.34\cdot10^{-10}$
$(0.8,0.8)$	$2.09\cdot10^{-2}$	$1.74\cdot10^{-4}$	$3.89\cdot10^{-7}$	$5.04\cdot10^{-10}$
$(0.9,0.9)$	$1.94\cdot10^{-2}$	$2.09\cdot10^{-4}$	$5.48\cdot10^{-7}$	$6.64\cdot10^{-10}$
$(1.0,1.0)$	$1.27\cdot10^{-2}$	$1.58\cdot10^{-4}$	$4.64\cdot10^{-7}$	$6.45\cdot10^{-10}$

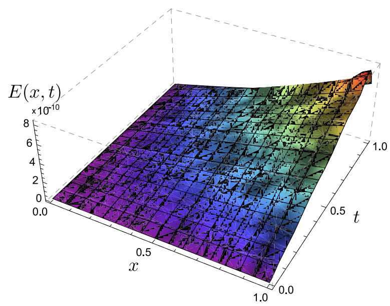

Figure 8. AE curve of Example 4 for $N=M=8$.

7 Conclusion

In this paper, the SJGC method was applied to solve the IDEs with the initial conditions. This method is very straight forward technique to solve the IDEs. SJGC method converts the IDE equation to a system of algebraic equations, which can be solved by usual numerical methods. In addition, the collocation treatments were introduced for the nonlocal condition. From the tables, numerical examples were given to confirm the rightness and reliability of the our method. The results display the SJC method is accurate.

References

1. W.M. Abd-Elhameed, E.H. Doha, Y.H. Youssri, Efficient spectral-Petrov-Galerkin methods for third and fifth-order differential equations using general parameters generalized Jacobi polynomials, *Quaest. Math.*, **36**:15–38, 2013.
2. M.A. Abdelkawy, S.S. Ezz-Eldien, A.Z.M. Amin, A Jacobi spectral collocation scheme for solving Abel's integral equations, *Progr. Fract. Differ. Appl.*, **1**(3):187–200, 2015.
3. B. Ahmad, S. Sivasundaram, On four-point nonlocal boundary value problems of nonlinear integro-differential equations of fractional order, *Appl. Math. Comput.*, **217**:480–487, 2010.
4. S. Akhavan, K. Maleknejad, Improving Petrov–Galerkin elements via Chebyshev polynomials and solving Fredholm integral equation of the second kind by them, *Appl. Math. Comput.*, **271**: 352–364, 2015.
5. A.H. Bhrawy, M.A. Abdelkawy, J. Tenreiro Machado, A.Z.M. Amin, Legendre–Gauss–Lobatto collocation method for solving multi-dimensional Fredholm integral equations, *Comput. Math. Appl.*, 2016, https://doi.org/10.1016/j.camwa.2016.04.011.
6. A.H. Bhrawy, D. Baleanu, A spectral Legendre–Gauss–Lobatto collocation method for a space-fractional advection diffusion equations with variable coefficients, *Rep. Math. Phys.*, **72**:219–233, 2013.
7. A.H. Bhrawy, E.H. Doha, D.Baleanu, S.S. Ezz-Eldien, A spectral tau algorithm based on Jacobi operational matrix for numerical solution of time fractional diffusion-wave equations, *J. Comput. Phys.*, **293**:142–156, 2015.
8. A.H. Bhrawy, M.A. Zaky, A method based on the Jacobi tau approximation for solving multi-term time-space fractional partial differential equations, *J. Comput. Phys.*, **281**:876–895, 2015.
9. A.H. Bhrawy, M.A. Zaky, A method based on the Jacobi tau approximation for solving multi-term time-space fractional partial differential equations, *J. Comput. Phys.*, **281**:876–895, 2015.
10. A.H. Bhrawy, M.A. Zaky, R.A. Van Gorder, A space-time Legendre spectral tau method for the two-sided space-time Caputo fractional diffusion-wave equation, *Numer. Algorithms*, **71**(1):151–180, 2016.
11. C. Canuto, M.Y. Hussaini, A. Quarteronia, T.A. Zang, *Spectral Methods: Fundamentals in Single Domains*, Springer, Berlin, Heidelberg, 2006.
12. A. Cardone, D. Conte, Multistep collocation methods for Volterra integro-differential equations, *Appl. Math. Comput.*, **221**:770785, 2013.
13. W.T. Chaolu, P. Jing, New algorithm for second-order boundary value problems of integro-differential equation, *J. Comput. Appl. Math.*, **299**:1–6, 2009.

14. J. Chen, Y. Huang, H. Rong, T. Wu, T. Zen, A multiscale Galerkin method for second-order boundary value problems of Fredholm integro-differential equation, *J. Comput. Appl. Math.*, **290**:633–640, 2015.

15. Y. Chen, J. Zhou, Error estimates of spectral Legendre–Galerkin methods for the fourth-order equation in one dimension, *Appl. Math. Comput.*, **268**:1217–1226, 2015.

16. Ş. Yüzbaşı, N. Şahin, M.Sezer, Numerical solutions of systems of linear Fredholm integro-differential equations with Bessel polynomial bases, *Comput. Math. Appl.*, **61**:3079–3096, 2011.

17. M. Dehghan, R. Salehi, The numerical solution of the non-linear integro-differential equations based on the meshless method, *J. Comput. Appl. Math.*, **236**:2367–2377, 2012.

18. E.H. Doha, M.A. Abdelkawy, A.Z.M. Amin, A.M. Lopes, On spectral methods for solving variable-order fractional integro-differential equations, *Comput. Appl. Math.*, **37**:3937–3950, 2018.

19. M.R. Eslahchi, M. Dehghan, M. Parvizi, Application of the collocation method for solving nonlinear fractional integro-differential equations, *J. Comput. Appl. Math.*, **257**:105–128, 2014.

20. F. Ghoreishi, S. Yazdani, An extension of the spectral tau method for numerical solution of multi-order fractional differential equations with convergence analysis, *Comput. Math. Appl.*, **61**:30–43, 2011.

21. B.-Y. Guo, Jacobi approximations in certain Hilbert spaces and their applications to singular differential equations, *J. Math. Anal. Appl.*, **243**:373–408, 2000.

22. Y. Jiang, J. Mab, Spectral collocation methods for Volterra integro-differential equations with noncompact kernels, *J. Comput. Appl. Math.*, **244**:115–124, 2013.

23. G. Kitzler, J. Schöberl, A high order space-momentum discontinuous Galerkin method for the Boltzmann equation, *Comput. Math. Appl.*, **70**:1539–1554, 2015.

24. S.R. Lau, R.H. Price, Sparse spectral-tau method for the three-dimensional helically reduced wave equation on two-center domains, *J. Comput. Phys.*, **231**:7695–7714, 2012.

25. J. Ma, Blow-up solutions of nonlinear Volterra integro-differential equations, *Math. Comput. Modelling*, **54**:2551–2559, 2011.

26. J. Ma, B.W. Li, J.R. Howell, Thermal radiation heat transfer in one and two-dimensional enclosures using the spectral collocation method with full spectrum k-distribution model, *Int. J. Heat Mass Transfer*, **71**:35–43, 2014.

27. X. Ma, C. Huang, Spectral collocation method for linear fractional integro-differential equations, *Appl. Math. Model.*, **38**:1434–1448, 2014.

28. F.M. Mahfouz, Numerical simulation of free convection within an eccentric annulus filled with micropolar fluid using spectral method, *Appl. Math. Comput.*, **219**:5397–5409, 2013.

29. K. Maleknejad, S. Akhavan, Using the improved Petrov–Galerkin elements $k - 0$ for solving nonlinear Hammerstein–Fredholm integral equations, *SIAM J. Numer. Anal.*, **267**:107–116, 2014.

30. K. Maleknejad, B. Basirat, E. Hashemizadeh, A Bernstein operational matrix approach for solving a system of high order linear Volterra–Fredholm integro-differential equations, *Math. Comput. Model.*, **55**:1363–1372, 2012.

31. K. Maleknejad, Y. Mahmoudi, Taylor polynomial solution of high-order nonlinear Volterra–Fredholm integro-differential equations, *Appl. Math. Comput.*, **145**(2–3):641–653, 2003.

32. P. Michaels, B. Zubik-Kowal, Parallel computations and numerical simulations for nonlinear systems of Volterra integro-differential equations, *Commun. Nonlinear Sci. Numer. Simul.*, **17**: 3022–3030, 2012.

33. A. Mohsen, M. El-Gamel, On the numerical solution of linear and nonlinear Volterra integral and integro-differential equations, *Appl. Math. Comput.*, **217**:3330–3337, 2010.

34. S.Y. Reutskiy, A new collocation method for approximate solution of the pantograph functional differential equations with proportional delay, *Appl. Math. Comput.*, **266**:642–655, 2015.

35. A. Saadatmandi, M. Dehghan, Numerical solution of the higher-order linear Fredholm integro-differential-difference equation with variable coefficients, *Comput. Math. Appl.*, **59**:2996–3004, 2010.

36. J. Saberi-Nadjafi, M. Tamamgar, The variational iteration method: A highly promising method for solving the system of integro-differential equations, *Comput. Math. Appl.*, **56**:346–351, 2008.

37. H. Saeedi, M.M. Moghadam, Numerical solution of nonlinear Volterra integro-differential equations of arbitrary order by CAS wavelets, *Commun. Nonlinear Sci. Numer. Simul.*, **16**: 1216–1226, 2011.

38. H. Saeedi, M.M. Moghadam, N. Mollahasani, G.N. Chuev, Numerical solution of nonlinear Volterra integro-differential equations of arbitrary order by CAS wavelets, *Commun. Nonlinear Sci. Numer. Simul.*, **16**:1154–1163, 2011.

39. P.K. Sahu, S. SahaRay, Legendre spectral collocation method for Fredholm integro-differential-difference equation with variable coefficients and mixed conditions, *Appl. Math. Comput.*, **268**:575–580, 2015.

40. H. Schamel, K. Elsässer, The application of the spectral method to nonlinear wave propagation, *J. Comput. Phys.*, **22**:501–516, 1976.

41. W. Shaoa, X. Wu, An effective Chebyshev tau meshless domain decomposition method based on the integration-differentiation for solving fourth order equations, *Appl. Math. Model.*, **39**: 2554–2569, 2015.

42. J. Shen, T. Tang, L.L. Wang, *SPECTRAL METHODS: Algorithms, Analyses and Applications*, Springer Ser. Comput. Math., Vol. 41, Springer, Berlin, Heidelberg, 2011.

43. T. Tang, X. Xu, J. Cheng, On spectral methods for Volterra integral equation and the convergence analysis, *J. Comput. Math.*, **26**(6):825–837, 2008.

44. X. Tang, Efficient Chebyshev collocation methods for solving optimal control problems governed by Volterra integral equations, *Appl. Math. Comput.*, **269**:118–128, 2015.

45. M. Turkyilmazoglu, High-order nonlinear Volterra–Fredholm–Hammerstein integro-differential equations and their effective computation, *Appl. Math. Comput.*, **247**:410–416, 2014.

46. Ş. Yüzbaş, N. Şahin, A. Yildirim, A collocation approach for solving high-order linear Fredholm–Volterra integro-differential equations, *Math. Comput. Model.*, **55**:547–563, 2012.

47. M. Zarebnia, Sinc numerical solution for the Volterra integro-differential equation, *Commun. Nonlinear Sci. Numer. Simul.*, **15**:700–706, 2010.